

Impact of ECCD on Alfvén Eigenmodes in the TJ-II stellarator

Á. Cappa¹, D. López-Bruna¹, J.L. Velasco¹, A. González-Jerez², J.M. García Regaña¹
 M. Ochando¹, S. Yamamoto³, M. Liniers¹, E. Ascasíbar¹, F. Castejón¹, J. M. Fontdecaba¹
 F. Medina¹, M. García Muñoz⁴, N. Marushchenko⁵

¹ Laboratorio Nacional de Fusión, Madrid, Spain

² Universidad Complutense de Madrid, Spain

³ Institute of Advanced Energy, Kyoto University, Japan, ⁴ Universidad de Sevilla, Spain

⁵ Max Planck Institut für Plasmaphysik, Greifswald, Germany

Introduction

This paper addresses the impact of Electron Cyclotron Current Drive (ECCD) on the Alfvén Eigenmodes (AEs) activity in low-shear stellarators. To this end, experiments have been carried out in the TJ-II stellarator NBI plasmas using ECRH on-axis with and without ECCD. To understand the changes observed in the AEs spectrum, the influence of the different contributions to the plasma current (NBED, ECCD, Bootstrap) on the rotational transform profile, and thus on the Shear Alfvén Spectrum (SAS), is investigated numerically by means of the STELLGAP [1] and AE3D [2] codes.

Experimental Results

TJ-II stellarator is equipped with two NBI injectors providing co and counter sub-Alfvénic H_0 beams ($v_{beam}/v_A \sim 0.2 - 0.3$ for line averaged densities around $0.5 \times 10^{19} \text{ cm}^{-3}$) which deliver up to 700 kW port-through power per injector. The experiments described in this paper have been carried out using only the co-direction injector in deuterium plasmas. Additionally, two 53.2

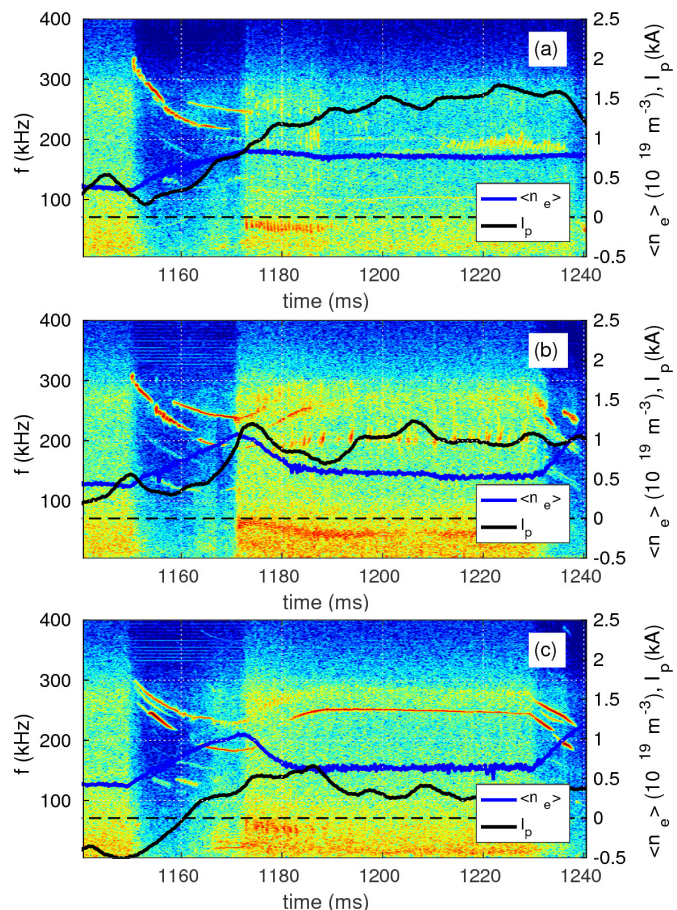


Figure 1: Magnetic fluctuations during NBI phase. Reference shot without ECRH (#44257, a); with ECRH and no ECCD (#44272, b) and with ECCD (#44274, c) are shown.

GHz gyrotrons, generating up to 250 kW of EC power each (second harmonic X-mode), create and heat the target plasma used for NBI injection. Fig. 1 shows the spectrogram of magnetic fluctuations observed when ECRH without (b) and with ECCD (c) is launched during the NBI phase. A reference shot without ECRH is also shown (a). In order to understand the influence of ECCD on the AEs activity we must first establish the impact of ECRH itself. As it is shown in Fig. 1 (b), plasma density and total plasma current during the NBI phase are both modified by the presence of on-axis ECRH power (from 1170 to 1230 ms). Obliquely launching this power with $N_{||} = 0.2$ drives an extra counter-current contribution which results in a strong change in the observed AEs (Fig. 1(c)). In this case, line density is the same, plasma profiles barely change (not shown here) and only the plasma current exhibits a significant modification ($\Delta I_p \approx -0.7$ kA) compared to the ECCD-free case.

Modelling

Using $n_e(\rho)$ and $T_e(\rho)$ measured by Thomson Scattering, $T_i(0)$ measured by NPA (where the profile $T_i(\rho)$ has been taken proportional to $n_e(\rho)$ in NBI+ECRH plasmas and to $T_e(\rho)$ in

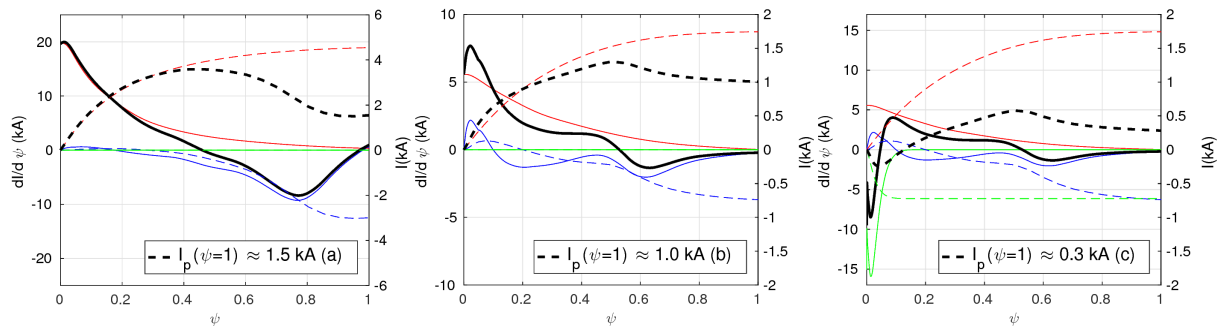


Figure 2: Bootstrap (blue), NBCD (red), ECCD (green) and total (black) integrated currents (dashed lines) and current densities (solid lines).

pure NBI plasmas [3]), we may calculate the bootstrap current [4], the ECCD current using the TRAVIS code [5] and obtain a rough approximation to the current driven by the neutral beam (NBCD) using the fast ion birth profile calculated with FAFNER [6], normalized to the experimental current. Fig. 2 shows the current densities $dI/d\psi$ (solid lines) associated to each contribution, as well as the integrated currents (dashed lines). The total current density is represented by the solid black line. The unknown NBCD amplitude on-axis is chosen such the integrated total plasma current at $\psi = 1$

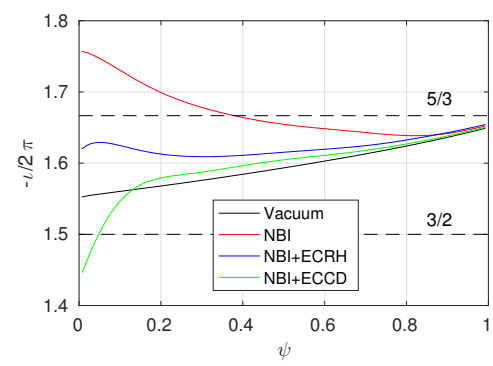


Figure 3: Rotational transform profiles.

corresponds approximately to the total experimental current measured at $t = 1200$ ms. The reference NBI shot (a) and the ECRH+NBI cases with (c) and without (b) ECCD are shown. Introducing in VMEC a polynomial fit to the total current density we obtain the iota profiles represented in Fig. 3. VMEC outputs, together with the density profiles of each shot, are then used to run STELLGAP in order to obtain the SAS, which is shown in Fig. 4 for the three experimental cases and the three mode families typical of a four period device. Toroidal mode

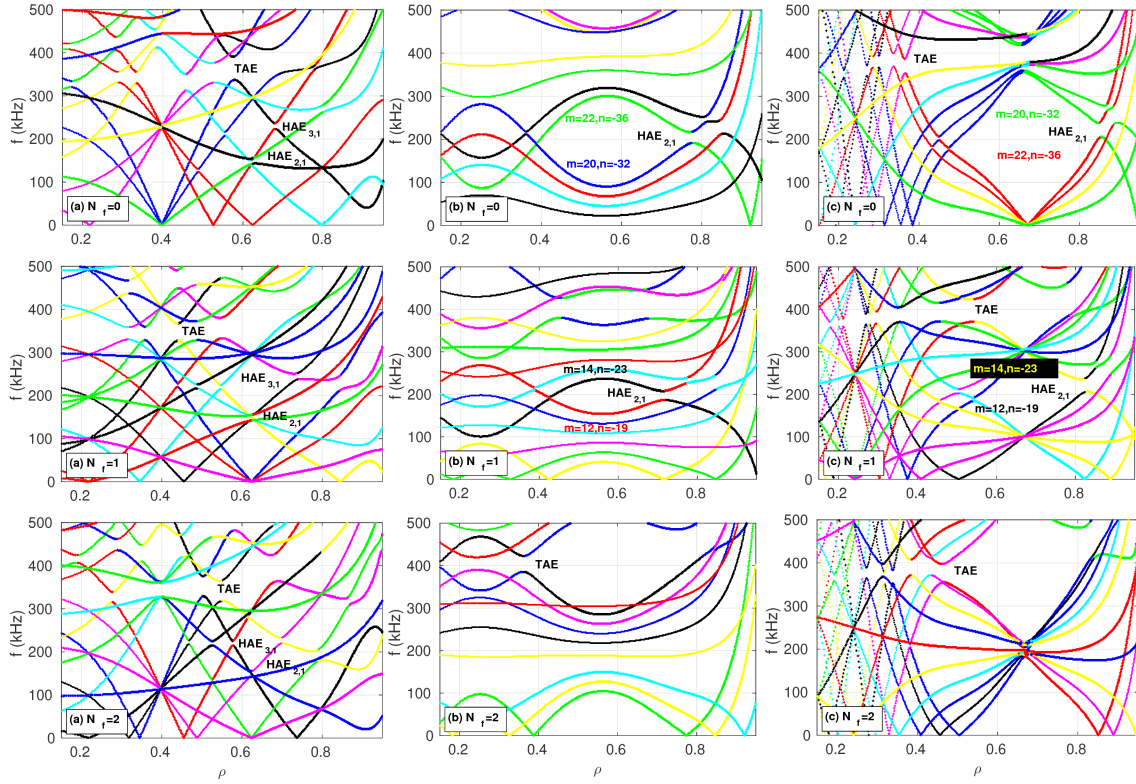


Figure 4: Shear Alfvén spectrum for $N_f = 0, -1, -2$. On the left the NBI reference case is shown (a). The NBI+ECRH (b) and NBI+ECCD cases (c) are plotted on the central and right panels respectively.

distribution from $n = -1$ to -36 (following TJ-II equilibrium convention with negative ι) and a maximum poloidal mode number $m = 25$, were considered. These numbers were determined using a previous calculation with a simple cylindrical model and limiting the theoretical mode frequency to values not far from the experimentally observed limit (400 kHz). Measured central densities around $n_e(0) = 1.1 \times 10^{19} \text{ m}^{-3}$ for the NBI case and $n_e(0) = 0.7 \times 10^{19} \text{ m}^{-3}$ for the NBI+ECRH and NBI+ECCD cases were used. An experimental ratio $D/H \approx 1.8$ was also measured in these shots and therefore an ion to proton mass ratio of 2 was preferably taken to perform the simulations. The result indicates that the steady frequency mode observed in Fig. 1 (c) could correspond to modes appearing in the $\text{HAE}_{2,1}$ gap. TAE gap is also predicted at higher frequencies but no activity at these high frequencies has been observed to date. Look-

ing at the structure of the SAS and comparing it to the magnetic fluctuations represented in Fig. 1 it appears that HAE_{2,1} gap becomes wider as the iota profile evolves from the pure NBI to the NBI+ECCD case, thus favoring the presence of the mode in the NBI+ECCD case.

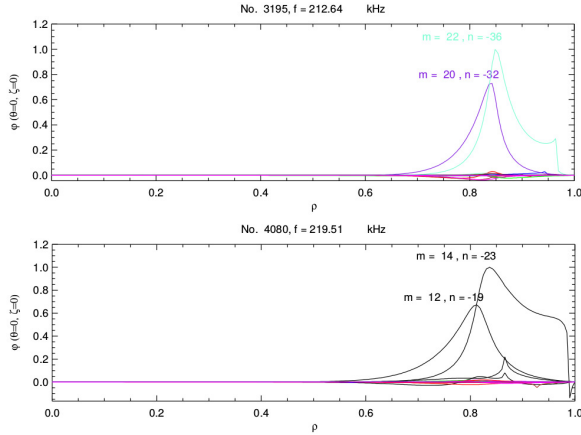


Figure 5: Dominant amplitudes for modes at $f \approx 213$ kHz and $f \approx 220$ kHz obtained with AE3D code.

current density calculations, which have not been included in the analysis, need to be assessed to check the robustness of the result. The same experiment with a very similar result was carried out using another ECRH beam located in a stellarator symmetric position.

Conclusion¹

ECCD is an effective tool to modify AEs activity in low shear devices. A small amount of driven current produces noticeable changes on the spectrum of observed modes. However, comparison with MHD theory is a difficult task since all the current contributions must be taken into account in order to model ι . Experimental determination of rotational transform profile using Motional Stark Effect (MSE) is foreseen in forthcoming experiments, helping to validate the current density estimation and improving the inputs of the MHD codes.

References

- [1] D.Spong, R. Sánchez and A. Weller, Phys. of Plamas **10**, 3217 (2003)
- [2] D.Spong, E. D'Azevedo and Y. Todo, Phys. of Plamas **17**, 022106 (2010)
- [3] J.M. Fontdecaba et al, Plasma Fusion Research **5**, S2085 (2010)
- [4] J.L. Velasco et al, Plasma Phys. Control. Fusion **53**, 115014 (2011)
- [5] N.B. Marushchenko, Y.Turkin and H.Maassberg, Comput. Phys. Commun. **185**, 165 (2014)
- [6] J. Guasp, M. Liniers, Fusion Tech. **24** 251 (1993)

¹This work has been carried out within the framework of the EUROfusion Consortium and has received funding from the Euratom research and training programme 2014-2018 under grant agreement N°633053. The views and opinions herein expressed do not necessarily reflect those of the European Commission. The work has been partially funded by task agreement VPENR:Enabling Research:Project AWP17-ENR-MFE-CIEMAT-03.

Fig. 5 shows the mode amplitudes calculated with AE3D for the dominant $m = 22, n = -36$ and $m = 20, n = -32$ ($N_f = 0$) and the $m = 14, n = -23$ and $m = 12, n = -19$ ($N_f = 1$) perturbations. Provided the mode identification is correct, the observed mode frequencies are approximately 15% higher than the predicted ones, probably because a deuterium ion mass has been used in the simulations. Given the high sensitivity of the SAS on ι variations, the uncertainties related to the